Causes of the Northern Gulf of Guinea Cold Event in 2012

C. Y. Da-Allada, J. Agada, E. Baloïtcha, M. N. Hounkonnou, J. Jouanno, G. Alory

JGR Oceans

RESEARCH ARTICLE
10.1029/2021JC017627

Causes of the Northern Gulf of Guinea Cold Event in 2012

C. Y. Da-Allada[1,2,3], J. Agada[2], E. Baloïtcha[2], M. N. Hounkonnou[2], J. Jouanno[4], and G. Alory[4]

[1]LaGEA/ENSTP/UNSTIM, Abomey, Benin, [2]ICMPA-UNESCO Chair/UAC, Cotonou, Bénin, [3]LHMC/IRHOB, Cotonou, Bénin, [4]CNES, CNRS, IRD, UPS, LEGOS, Université de Toulouse, Toulouse, France

Key Points:

- Causes of the anomalous cooling seen in the northern Gulf of Guinea coast between February and June 2012 are investigated
- Sea Surface Temperature anomalies were important in the coastal upwelling regions of Sassandra in Côte d'Ivoire and Takoradi in Ghana
- Sassandra cooling was due to vertical mixing and zonal advection changes, whereas only meridional advection changes caused Takoradi cooling

Correspondence to:
C. Y. Da-Allada,
daallada@yahoo.fr

Citation:
Da-Allada, C. Y., Agada, J., Baloïtcha, E., Hounkonnou, M. N., Jouanno, J., & Alory, G. (2021). Causes of the northern Gulf of Guinea cold event in 2012. *Journal of Geophysical Research: Oceans*, *126*, e2021JC017627. https://doi.org/10.1029/2021JC017627

Received 1 JUN 2021
Accepted 26 JUL 2021

Abstract Particularly cool sea surface temperatures (SSTs) were observed in 2012 along the Northern Gulf of Guinea coast. This strong cooling event was seen from February to June and reached maxima in the coastal upwelling areas: SST anomalies of −1°C were observed in Sassandra Upwelling area in Côte d'Ivoire (SUC, situated east of Cape Palmas) and SST anomalies of −0.5°C were observed in Takoradi Upwelling area in Ghana (TUG, located east of Cape Three Points). In SUC and TUG regions, the 2012 decrease in SST was the coldest event recorded over the 1990–2018 period (29 years). From the analysis of regional simulations, we show that the mechanisms behind this SST decrease differ in the two regions. In the SUC region, we identify changes in both zonal advection (related to zonal SST gradient changes) and increased vertical mixing as the main drivers of the anomalous cooling. The anomalous vertical mixing is linked to increased vertical shear of the zonal current in response to the Guinea Current strengthening. In the TUG region, acceleration of the southward advection of the surface water, due to the intensification of the meridional Ekman current generated by the strengthening of the zonal wind stress, was identified as the major cause of the SST anomalous cooling.

Plain Language Summary We investigate the causes of the anomalous cooling that happened in the northern Gulf of Guinea coast between February and June 2012 using observations and model data. The abnormal sea surface temperature decrease was pronounced at the upwelling regions of Sassandra in Côte d'Ivoire and Takoradi in Ghana. Results reveal that the anomalous cooling, in the Sassandra upwelling area, was mainly due to changes in both the vertical mixing at the base of mixed layer and zonal advection, whereas only changes in meridional advection explained the anomalous cooling seen in the Takoradi upwelling area.

1. Introduction

Located in the eastern equatorial Atlantic Ocean (15°W–15°E, 10°S–8°N), the Northern Gulf of Guinea (NGoG; Figure 1) is marked by the presence of a seasonal coastal upwelling that peak twice a year, in boreal winter (January to February) and summer (June to October) periods, from Côte d'Ivoire to Nigeria (e.g., Djakouré et al., 2014, 2017; Sohou et al., 2020). The sea surface temperature (SST), widely used to characterize coastal upwelling in the NGoG, is subject to year-to-year variations that could affect the marine ecosystem (e.g., Binet & Marchal, 1993; Koné et al., 2017) and the onset of the West African monsoon (e.g., Ali et al., 2011; Lamb, 1972). Thus, interannual variability of the SST in the NGoG (although less pronounced than the seasonal cycle) may exert a significant role on the regional climate (Gu & Adler, 2004; Kouadio et al., 2013; Opoku-Ankomah & Cordery, 1994).

Previous studies have demonstrated that areas of maximum SST interannual variability in the NGoG are those where the amplitude of the seasonal cycle is large (e.g., the seasonal upwelling regions) and the year-to-year SST variability is characterized by both warm and cold years (e.g., Hardman-Mountford & McGlade, 2003; Picaut, 1983; Toualy et al., 2012). It has been shown that local and/or nonlocal processes are important to explain interannual SST anomalies of the region (e.g., Servain et al., 1982; Wade et al., 2011). Regarding local processes, Wade et al. (2011) suggested that changes in vertical mixing is the main process controlling SST anomalies in the NGoG. The vertical mixing in this region is controlled by the vertical shear of current, which is driven by the strength of the Guinea Current (Jouanno et al., 2011). The crucial role of interannual variability of the wind stress in SST changes in the NGoG is also mentioned by Jouanno et al. (2017). The remote forcing (non local processes) is associated with the main mode of interannual variability of the equatorial Atlantic generally described as Atlantic Equatorial mode or Atlantic Niño mode

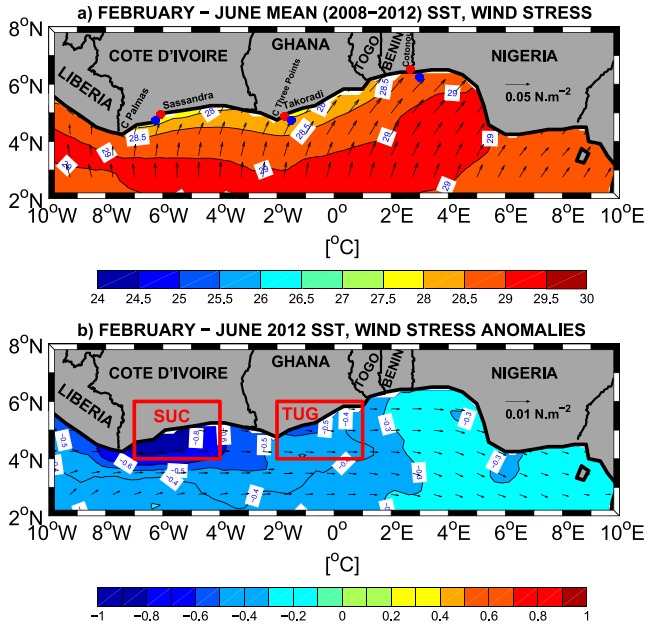

Figure 1. (a) Mean (2008–2012) February–June Optimum Interpolation-sea surface temperature (in °C; color shading) and ERA-Interim (ERAI) wind stress (in N.m^{-2}; vectors). The red dots represent the position of the PROPAO network ONSET thermometers deployed along the coast at Sassandra (6.08°W; 4.95°N), Takoradi (1.73°W; 4.88°N) and Cotonou (2.67°E; 6.52°N). The blue dots represent the Nucleus for European Modeling of the Ocean model grid points that are closest to the ONSET positions. (b) February–June 2012 anomalies (with respect to 2008–2012 mean seasonal cycle) of sea surface temperature and ERAI wind stress. As in Foltz and McPhaden (2006a), here and in subsequent figures, anomalies have been smoothed with two passes of a 3-month running mean filter. Boxes shown in (b) indicate the two regions of focus of this study.

(e.g., Foltz & McPhaden, 2010; Zebiak, 1993). This mode, which peaks in boreal summer (June-July-August), is characterized by a particularly strong irregular warming (cooling) of the SST in the Gulf of Guinea related to a weakening (strenghtening) of trade winds in the western equatorial region (e.g., Foltz & McPhaden, 2010; Lübbecke & McPhaden, 2013). In the NGoG, some strong warm or cold SST events are linked to the Atlantic Niño mode (e.g., Hardman-Mountford & McGlade, 2003). Apart from the equatorial mode, the Atlantic meridional mode or Atlantic dipole, may also be involved in the Gulf of Guinea SST anomalies (Burmeister et al., 2016; Chang et al., 1997; Foltz & McPhaden, 2010). The Atlantic meridional mode is defined by an anomalous meridional SST gradient with opposite anomalies north and south of the thermal equator (~5°N), and appears in boreal spring (March-April-May). This mode is thought to be largely controlled by thermodynamics through wind-induced evaporation and positive wind-evaporation-SST feedback (Chang et al., 1997, 2001; Foltz & McPhaden, 2010).

Recently, Sohou et al. (2020) found strong negative SST anomalies during 2012 in the NGoG, using the ONSET sensor data series deployed in three stations (Sassandra in Côte d'Ivoire, Takoradi in Ghana and Cotonou in Benin) along the northern coast of Gulf of Guinea over the period 2008–2012. Their study did not examine the mechanisms behind this cooling. They suggested that it may be related to interannual Atlantic climatic modes.

The main objective of this study is to investigate the causes of the 2012 anomalous cooling in the NGoG, using observations and a regional numerical simulation of the Tropical Atlantic Ocean. The rest of the manuscript is organized as follows: observations, model description and the methodology used in this study are described in Section 2. Results including the observed cold SST event during 2012, evaluation of model and the mechanisms associated with the 2012 SST cooling in the NGoG are presented in Section 3. Finally, a summary and discussion are given in Section 4.

2. Observations, Model and Methods

2.1. Observations Data

We use three different sources of SST to document the cold event seen in 2012 in the NGoG. The first product is the monthly Optimum Interpolation SST (OI-SST) provided by the National Oceanic and Atmospheric Administration (NOAA), which combines satellite and in situ observations with a horizontal resolution of 1/4° and available from 1982 to present (Reynolds et al., 2002, 2007). The second product is the monthly SST ERA-Interim (ERAI) reanalysis product available at 0.75° resolution and from 1979 to 2019. ERAI product is derived from the European Center for Medium Range Weather Forecasts (ECMWF) (Dee et al., 2011). The last product of SST used is based on three coastal stations equipped with ONSET sensors installed along the NGoG coast at Sassandra (6.08°W; 4.95°N), Takoradi (1.73°W; 4.88°N) and Cotonou (2.67°E; 6.52°N) in the framework of the Research Program in Physical Oceanography in West Africa (PROPAO). The in situ ONSET sensor data series are available over the period 2008–2012 (Sohou et al., 2020). The period 2008–2012, when all data sets are available, is used for the study period. Interannual anomalies are calculated with respect to 2008–2012 mean seasonal cycle. As in Foltz and McPhaden (2006a), anomalies have been smoothed with two passes of a 3-month running mean filter.

2.2. Model

The model used is based on the Nucleus for European Modeling of the Ocean program (NEMO3.6, Madec and NEMO Team, 2016) and solves the three-dimensional primitive equations. The regional configuration

used has a horizontal resolution of 1/4°, covers the tropical Atlantic (35°S–35°N and 100°W–20°E) and provides daily outputs. On the vertical, there are 75 vertical levels, with 12 in the upper 20 m and 24 in the upper 100 m. A third-order upstream biased scheme which includes an implicit diffusion is used for momentum advection. Tracer advection is obtained using a total variance dissipation scheme and tracer diffusion is parameterized using a laplacian isopycnal operator with a coefficient of 300 $m^2.s^{-1}$. A Generic Length Scale scheme with a k-ε turbulent closure is used for the vertical diffusion coefficient (Reffrary et al., 2015; Umlauf & Burchard, 2003).

The lateral boundaries conditions are extracted from the daily outputs of the global Mercator reanalysis GLORYS2V3 (GLobal Ocean ReanalYSes and Simulations version 3; Ferry et al., 2012). At the surface, atmospheric fluxes are given by bulk formulae (Large & Yeager, 2009) and forced with the Drakkar Forcing Set version 5.2 (DFS5.2) product (Dussin et al., 2016). The monthly climatology of river runoffs from Dai and Trenberth (2002) is prescribed near the river mouths as a surface freshwater flux. The simulation is run from 1958-2015 and daily averages from 2008 to 2012 are analyzed in this study. For more details concerning the parameterization and some elements of validation, including comparisons with in situ observations, the reader is referred to Jouanno et al. (2011) and Hernandez et al. (2016) for temperature and mixed-layer depth (MLD), and Da-Allada et al. (2014, 2017) for sea surface salinity variations in the Gulf of Guinea.

2.3. Model Mixed-Layer Heat Budget

To examine the causes of the anomalously cold SST in 2012, we used the mixed-layer heat budget which can be written as follows (see Vialard et al., 2001, or Jouanno et al., 2011, 2017):

$$\frac{\partial \langle T \rangle}{\partial t} = \underbrace{\frac{Q_{\mathrm{ns}} + Q_s\left(1 - f_{z=-h}\right)}{\rho_0 C_p h}}_{\mathrm{NHF}} \underbrace{-\underbrace{\langle u.\partial_x T \rangle}_{\mathrm{XAD}} - \underbrace{\langle v.\partial_y T \rangle}_{\mathrm{YAD}}}_{\mathrm{HAD}} \underbrace{\underbrace{-\underbrace{\langle w.\partial_z T \rangle}_{\mathrm{ZAD}} - \underbrace{\frac{\left(k_z \partial_z T\right)_{z=-h}}{h}}_{\mathrm{ZDF}} - \underbrace{\frac{1}{h}\frac{\partial h}{\partial t}\left(\langle T \rangle - T_{z=-h}\right)}_{\mathrm{ENT}}}_{\mathrm{VER}} + \underbrace{D_l\left(T\right)}_{\mathrm{LDF}}}_{} \tag{1}$$

with

$$\langle \bullet \rangle = \frac{1}{h}\int \bullet \partial z \tag{2}$$

here, T is the model potential temperature, ρ_0 the surface reference density (set to 1,021 $kg.m^{-3}$ as in Li et al., 2013), C_p the heat capacity (set to 3984 J kg^{-1} °C^{-1} as in Wade et al., 2011), h the MLD, Q_{ns} the non-solar surface heat flux (sum of the net longwave radiation, the sensible and latent heat fluxes), Q_s the net shortwave radiation, $f_{z=-h}$ the fraction of the shortwave radiation that reaches the MLD, (u, v, w) the velocity components, K_z the vertical diffusion coefficient for tracers and $D_l(T)$ the lateral diffusion operator. The total temperature tendency on the left-hand side of (Equation 1) is thus driven from left to right by the storage of net air-sea heat flux (NHF) in the mixed-layer; horizontal advection (HAD) including zonal and meridional advection (XAD and YAD, respectively); vertical processes (VER) including the vertical advection (ZAD), the vertical diffusion (ZDF) and the entrainment (ENT) at the base of the mixed-layer; and finally the lateral diffusion (LDF). Hereafter, we define oceanic processes under the term OCP (OCP = HAD + VER + LDF). Note that all terms in Equation 1 are computed explicitly in the model except for the ENT term which is estimated as a residual. The MLD is defined as the depth where the density increase compared to density at 10 m equals 0.03 kg m^{-3}. The density criterion used to calculate MLD is the one recommended by de Boyer Montégut et al. (2004) and previously used in several studies in the region (e.g., Alory et al., 2021; Da-Allada et al., 2014; Jouanno et al., 2011, 2017). However, this criterion does not take into account the (rare) cases where the MLD is shallower than 10 m. The meridional current V is decomposed into geostrophic and Ekman components. The surface meridional Ekman velocity is computed as:

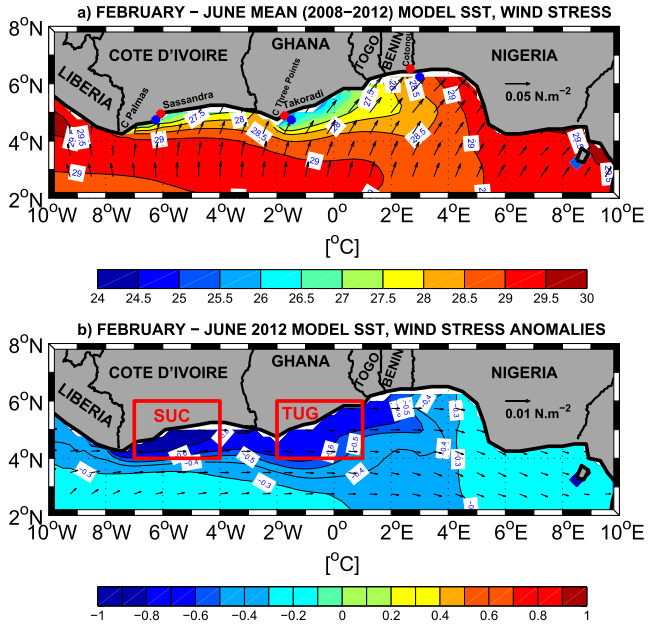

Figure 2. Same as Figure 1 but for the model.

$$V_{ek} = \frac{-\tau^x}{\rho_0 fh} \tag{3}$$

where τ^x is the zonal wind stress, f is the Coriolis parameter and the reference seawater density ρ_0. Then, the meridional geostrophic velocity is deduced from the difference between total meridional velocity and meridional Ekman velocity. The Brunt-Vaisala frequency $N^2(T,S)$ is used to describe the stratification due to temperature $N^2(T)$ and salinity $N^2(S)$ and is calculated as follows (e.g., Da-Allada et al., 2017):

$$N^2(T,S) = -\frac{g}{\rho}\frac{\partial \rho}{\partial z} \approx \left(\underbrace{g\alpha \frac{\partial T}{\partial z}}_{N^2(T)} - \underbrace{g\beta \frac{\partial S}{\partial z}}_{N^2(S)} \right) \tag{4}$$

with α the thermal expansion coefficient, β the haline contraction coefficient, g the gravity and ρ the density. The vertical shear squared Sh^2 due to zonal Shu^2 and meridional Shv^2 currents is used with the $N^2(T,S)$ determined above to explain ZDF term. The vertical shear squared is expressed as follows (e.g., Da-Allada et al., 2017):

$$\mathrm{Sh}^2 = \underbrace{\left(\frac{\partial u}{\partial z}\right)^2}_{\mathrm{Shu}^2} + \underbrace{\left(\frac{\partial v}{\partial z}\right)^2}_{\mathrm{Shv}^2} \tag{5}$$

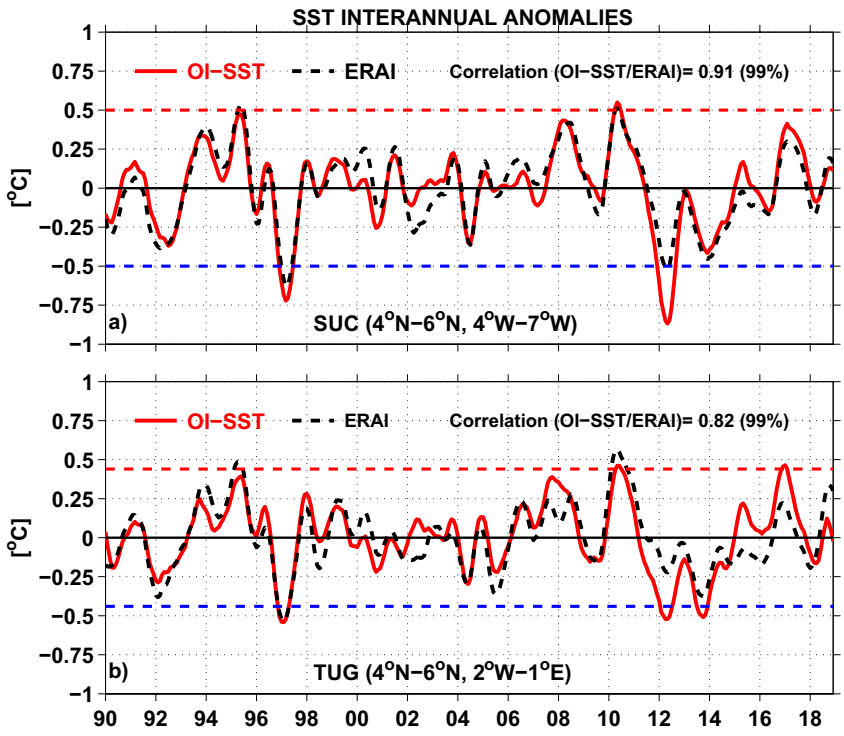

Figure 3. Time series of sea surface temperature (in °C) interannual monthly anomalies (with respect to 1990–2018 mean seasonal cycle) for the Optimum Interpolation-sea surface temperature (OI-SST) (red) and the ERA-Interim (ERAI) (dashed black) averaged in the regions of (a) Sassandra Upwelling area in Côte d'Ivoire and (b) Takoradi Upwelling area in Ghana (see Figure 1 for boxes locations). The red (blue) dotted line represents $+2\sigma$ (-2σ) of the series. σ is the standard deviation and its calculation is based on the filtered OI-SST data. The correlation coefficient between OI-SST and ERAI for the 1990–2018 period is indicated in each panel. The significance value of each correlation is also shown in each panel in the parentheses.

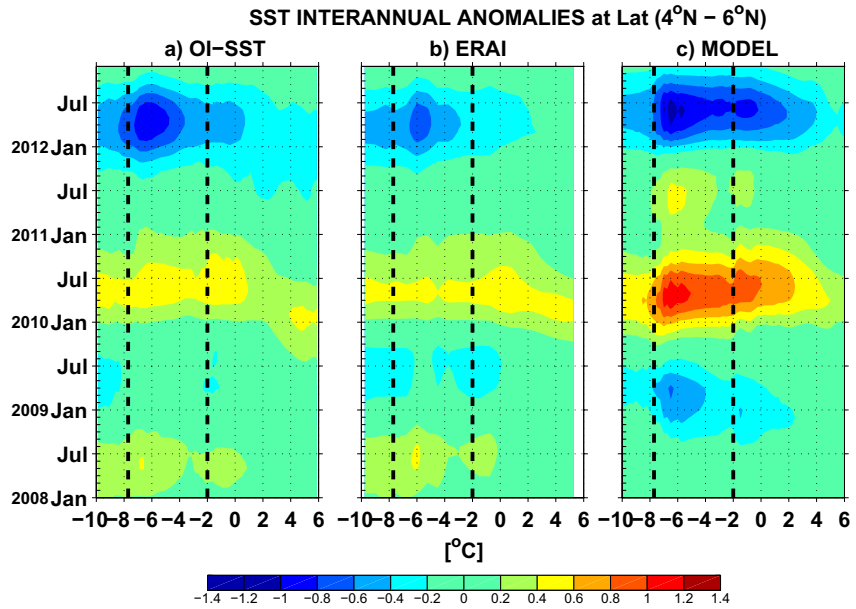

Figure 4. Longitude-time diagrams of the sea surface temperature anomalies averaged between 4°N and 6°N during January 2008–December 2012 for (a) Optimum Interpolation-sea surface temperature, (b) ERA-Interim and (c) Nucleus for European Modeling of the Ocean model. The dashed black line at 7.7°W (2°W) represents the longitude of Cape Palmas (Cape Three Points). Here and in subsequent figures, anomalies are calculated with respect to the 2008–2012 mean climatology. The units are °C.

3. Results

3.1. Observed Cold SST Event During 2012 and Model Evaluation in the NGoG

The OI-SST data revealed that the pronounced cold SST anomalies in 2012, already observed from the three coastal stations shown by Sohou et al. (2020), actually extended over the whole NGoG region (Figure 1). The peak SST anomalies occurred between February and June, which correspond to the climatological seasonal SST maximum (SST > 27.5°C). These anomalies are largest in the coastal upwelling regions of Sassandra in Côte d'Ivoire (around −1°C) and Takoradi in Ghana (close to −0.5°C; Figure 1). In these coastal upwelling areas, the negative SST anomalies seen in 2012 were the strongest during the 1990–2018 (29 years) period (Figure 3) and reached values greater than twice the standard deviation (2 × 0.25°C) of the series from January to October at the east of Cape Palmas in the area of Sassandra Upwelling in Côte d'Ivoire (SUC; 4°N–6°N, 4°W–7°W). These negative SST anomalies also reach twice the standard deviation (2 × 0.22°C) of the series in February-July at the east of Cape of the Three Points in the area of Takoradi Upwelling in Ghana (TUG; 4°N–6°N, 2°W–1°E). In the TUG region, the OI-SST data shows a cooling of the SST in 2012 similar to that obtained in 1997. Although OI-SST and ERAI are strongly correlated in the two regions (Figure 3), SST anomalies are more pronounced in OI-SST than ERAI. It has been shown that the OI-SST product reproduces SST variations better than ERAI in these regions (Sohou et al., 2020). The SUC and TUG regions selected are similar to those used by Roy (1995) and these two boxes are also bounded to capture the areas of strong SST cooling observed in 2012. During February–June 2012, the prevailing southwesterly winds in the NGoG were anomalously strong everywhere due to the zonal wind stress component (Figures 1a and 1b). As it will be shown below, these wind anomalies play a major role in the formation of the cold SST event in 2012. The results based on the model are similar to those obtained with the observations (Figure 2). However, SST anomalies are more important in the model than those obtained with the observations.

A time-longitude plot of SST anomalies averaged between 4°N and 6°N in the OI-SST data shows two major SST events over the 2008-2012 study period (Figure 4a): a strong cooling recorded in 2012 with anomalies reaching –1°C from February to June and a large SST warming (anomalies around + 0.5°C) during March–June 2010. The OI-SST data also show that the cooling that reached a peak in 2012 has started in October

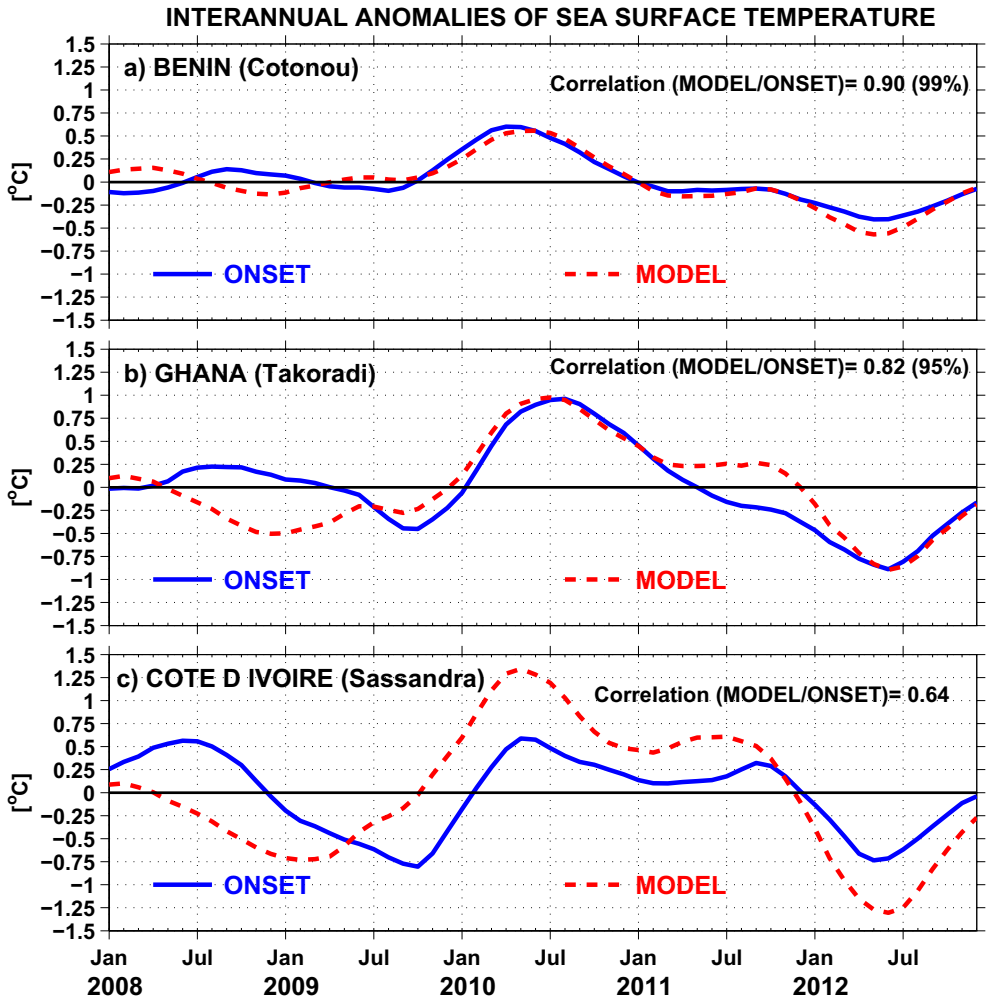

Figure 5. Interannual anomalies of sea surface temperature obtained from ONSET sensors (blue) and the model (dashed red) in the countries of the PROPAO network, that is in (a) Benin (Cotonou), (b) Ghana (Takoradi) and (c) Côte d'Ivoire (Sassandra). The distance between the ONSET sensor location and the nearest grid point of the model is ~48 km for Benin and ~30 km for Ghana and Côte d'Ivoire. The correlation coefficients of model against ONSET data for the study period are indicated in each panel. The significance value of each correlation is shown in the parentheses. The units are °C.

2011. These SST anomalies extended along the coast of the NGoG and were more pronounced at the east of Cape Palmas (Côte d'Ivoire) than at the east of Cape of the Three Points (Ghana). The important SST anomalies observed with the OI-SST data were also detected in the ERAI reanalysis product and the NEMO model used in this study (Figures 4b and 4c). However, ERAI exhibited slightly weaker SST anomalies while the model shows stronger SST anomalies than OI-SST. The model also displayed a cooling of SST (anomalies around −0.5°C) in early 2009 present but barely visible in the observations. The differences between the observations and model could be related to uncertainties in model forcing and/or model parameterization.

To reinforce the model evaluation, the simulated interannual SST anomalies are compared to ONSET in situ SST at the coastal stations (Figure 5). The model compares well with the ONSET data and shows the two major SST events of the study period mentioned above, namely the 2010 warming and the strong cooling of 2012. The magnitudes of the SST warm and cool anomalies in the model are similar to those of the ONSET data in Benin (Figure 5a) and Ghana (Figure 5b), while in Côte d'Ivoire, the SST anomalies are about twice stronger in the model than in ONSET (Figure 5c). Note also that in Côte d'Ivoire, the strong cooling in 2009 of ~ −0.75°C is shifted by 6 months in the model compared to ONSET. The difference between the ONSET SST anomalies values and the model in Sassandra (Côte d'Ivoire) could be explained by the intermediate

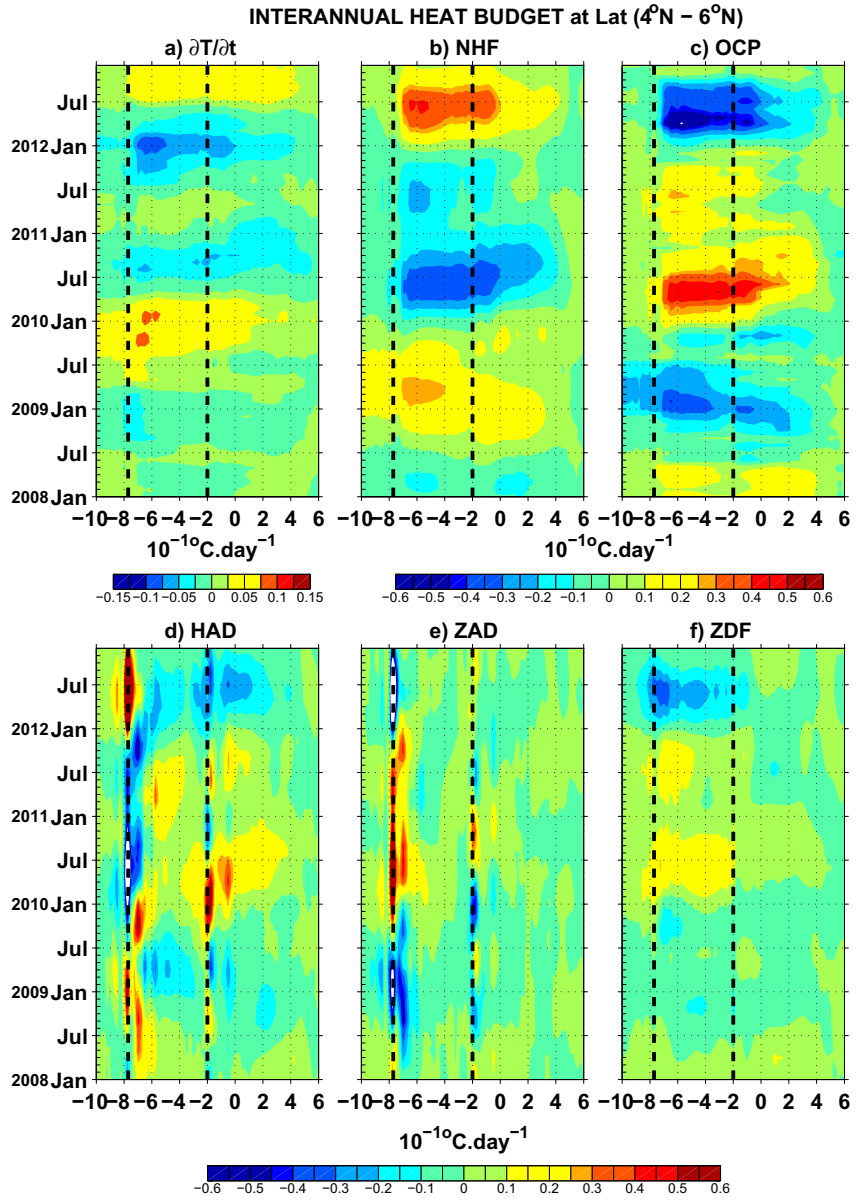

Figure 6. Longitude-time diagrams of anomalies of the main contributors to the mixed-layer heat budget averaged between 4°N and 6°N during January 2008–December 2012: (a) total mixed-layer temperature tendency, (b) net air-sea heat flux(NHF), (c) oceanic processes (OCP), (d) horizontal advection (HAD), (e) vertical advection (ZAD) and (f) vertical diffusion (ZDF). As in Figure 4, the dashed black line at 7.7°W (2°W) represents the longitude of Cape Palmas (Cape Three Points). The units are °C. day^{-1}. Note that the color scale in (a) is different from those of the other figures.

resolution of the model (1/4°) that may not allow to catch the full complexity of the coastal dynamics. It is important to mention that the interannual variability of SST was more pronounced in Ghana and Côte d'Ivoire than in Benin, in both observations and model.

Previous studies have discussed the SST warming observed in 2010 and have shown that it was not only observed in the NGoG but over the whole tropical Atlantic basin with the maximum SST anomalies near the African coast, near 20°N (Lefèvre et al., 2013). These authors have established that the increase in SST seen in 2010 was related to the weakening of the trade winds. Thus, we focus our study on the origin of the 2012 SST cold event in the NGoG only.

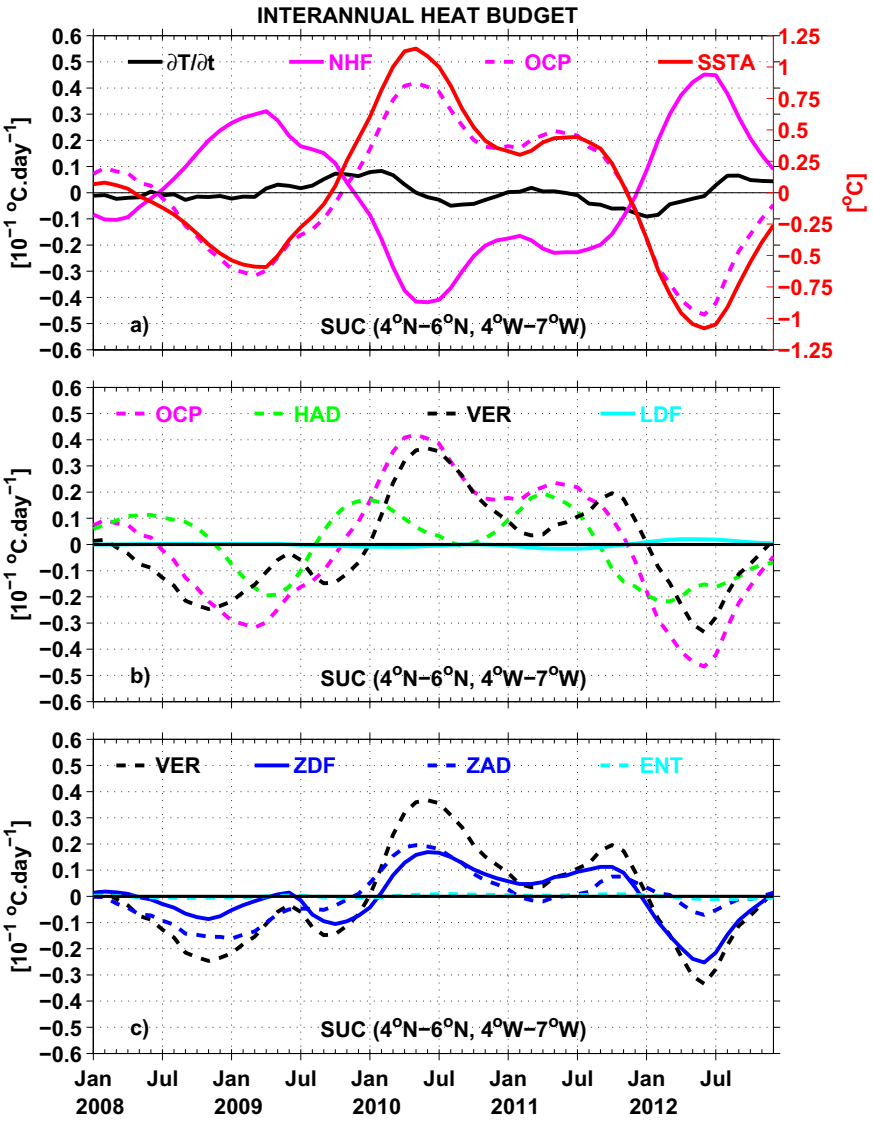

Figure 7. Interannual anomalies for 2008–2012 for the mixed-layer heat budget in the Sassandra Upwelling area in Côte d'Ivoire region: (a) total temperature tendency (black), net air-sea heat flux (NHF, magenta), oceanic processes (OCP, dashed magenta) and SST anomalies (SSTA, red). (b) Decomposition of oceanic processes: oceanic processes (dashed magenta, same as the dashed magenta line in (a), horizontal advection (HAD, dashed green), vertical processes (VER, dashed black), and lateral diffusion (LDF, light blue). (c) Decomposition of vertical processes: vertical processes (dashed black, same as the dashed black line in b), vertical diffusion (ZDF, blue), vertical advection (ZAD, dashed blue), and entrainment (ENT, dashed light blue). All terms are in °C. day^{-1}.

3.2. Mechanisms Associated With the 2012 SST Cooling in the NGoG

To identify the causes of the SST cooling in 2012, the time-longitude plots of total temperature tendency, net air-sea heat flux (NHF) and oceanic processes (OCP) are shown in Figures 6a–6c. There was a large interannual amplitude in the NHF, which was very similar to that of OCP (Figures 6b and 6c). These two terms were opposed one another most of the time leading to very weak interannual amplitude of the total temperature tendency (Figure 6a). The contribution of NHF was strongly positive (~+0.045°C.day^{-1} highest value over the study period) in 2012 whereas that of OCP was strongly negative (~−0.06°C.day^{-1} lowest value over the entire study period). Therefore, we deduce that the causes of the SST cooling observed in 2012 were controlled by OCP, which were dominated by changes in horizontal advection (HAD), vertical advection (ZAD) and vertical diffusion (ZDF) at the base of the mixed-layer (Figures 6d–6f). The 2012 cooling

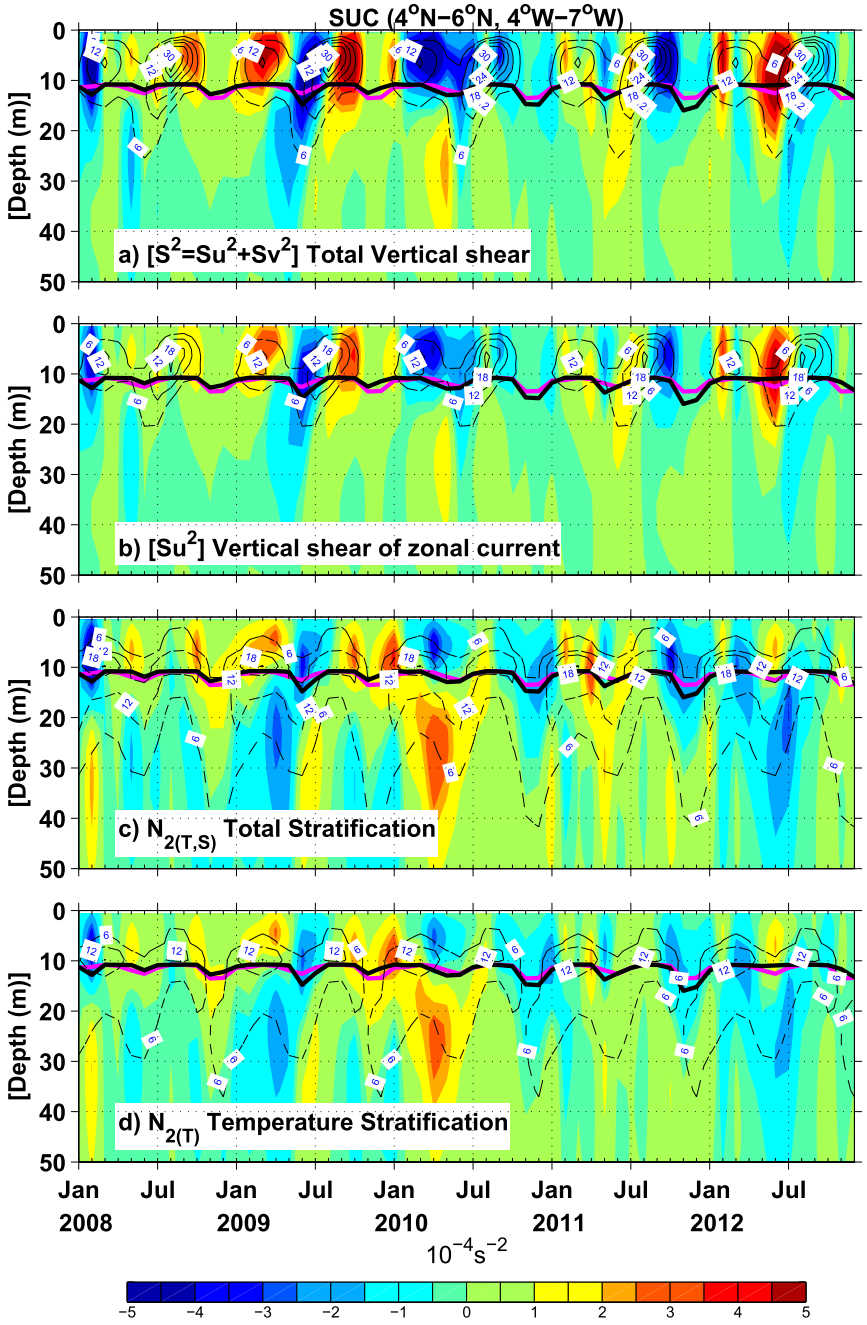

Figure 8. Interannual evolution of model vertical profiles for the 2008–2012 period in the Sassandra Upwelling area in Côte d'Ivoire region: (a) anomalies for total vertical shear in color (Sh^2, in 10^{-4} s^{-2}) and the climatology for the total vertical shear of the horizontal currents in black contours (every 4.10^{-4} s^{-2}) and, (b) same as (a) but for the vertical shear of zonal current, (c) same as (a) but for the total stratification $N^2_{(T,S)}$ and (d) same as (a) but for the temperature stratification $N^2_{(T)}$. The thick black line is the monthly evolution of the mixed-layer depth (MLD) during 2008–2012 and the thick magenta line represents the climatology of the MLD during 2008–2012.

seen in the NGoG was explained by changes in HAD and ZDF east of Cape Palmas (Côte d'Ivoire), whereas only changes in HAD were responsible for the 2012 cooling east of Cape Three Points (Ghana). To go further into the causes of the cold SST in 2012, we focus the rest of the analyses on the two regions SUC and TUG mentioned above and displayed in Figure 1.

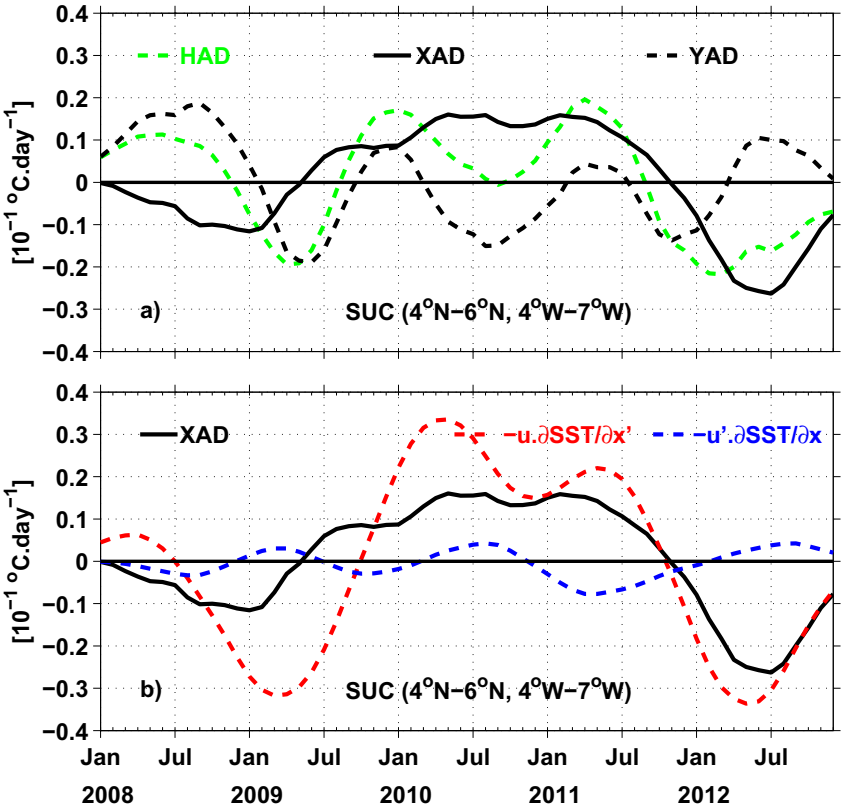

Figure 9. (a) Interannual anomalies for 2008–2012 in the Sassandra Upwelling area in Côte d'Ivoire region for (a) decomposition of horizontal advection (HAD, dashed green) into zonal (XAD, black) and meridional (YAD, dashed black) components and, (b) zonal advection (black, same as the black line in (a), zonal advection anomaly caused by the zonal sea surface temperature (SST) gradient anomalies (dashed red) and zonal advection anomaly created by the zonal current anomalies (dashed blue). All terms are in °C. day^{-1}.

In the SUC region, anomalous SST cooling was most intense between the end of 2011 and mid-2012, resulting in maximum SST anomalies of ∼ −1°C in June 2012 (Figure 7a). Note that in 2012 the 20°C isotherm depth was shallower than usual and the sea surface height showed a relative minimum at the same time, while not the largest of the 2008–2012 period (not shown). This suggests that there is no direct link between the SST cooling and change in upwelling strength. As mentioned above, both NHF and OCP terms displayed large interannual fluctuations and were of opposite signs thus leading to a very weak total tendency of temperature (Figure 7a). The OCP term was strongly correlated ($r = +0.98$, significant at the 99% level) with the SST interannual anomalies, which strongly suggests it controlled them. During 2012, NHF was positive while OCP was negative, which confirms that OCP caused the SST cooling seen at SUC. The OCP term was dominated by the vertical processes (VER) and HAD (Figure 7b). These two terms were both negative in 2012 and were responsible for the SST cold event. The SST cooling was initiated by HAD a couple of months before VER took over with a larger contribution.

Changes in VER were mainly driven by the ZDF (Figure 7c). Figure 8 shows that in the SUC region, the total vertical shear was controlled by vertical changes in zonal velocity (Figures 8a and 8b) and the total stratification was dominated by the temperature stratification (Figures 8c and 8d). In 2012, the SST cooling due to ZDF was explained by a strengthening of the vertical shear (positive anomalies) in the presence of a weak stratification (negative anomalies) at the base of the mixed-layer. In the SUC region, the shear was driven by the intensification of the Guinea Current (Jouanno et al., 2011). We indeed found an acceleration of the Guinea Current during the February–June 2012 period (not shown) leading to this enhanced shear. Note that, during February–June 2012 (the SST cooling period), the seasonal deepening of the MLD in June was absent and it was shallower than usual. The rest of the year 2012, the MLD showed very little departure

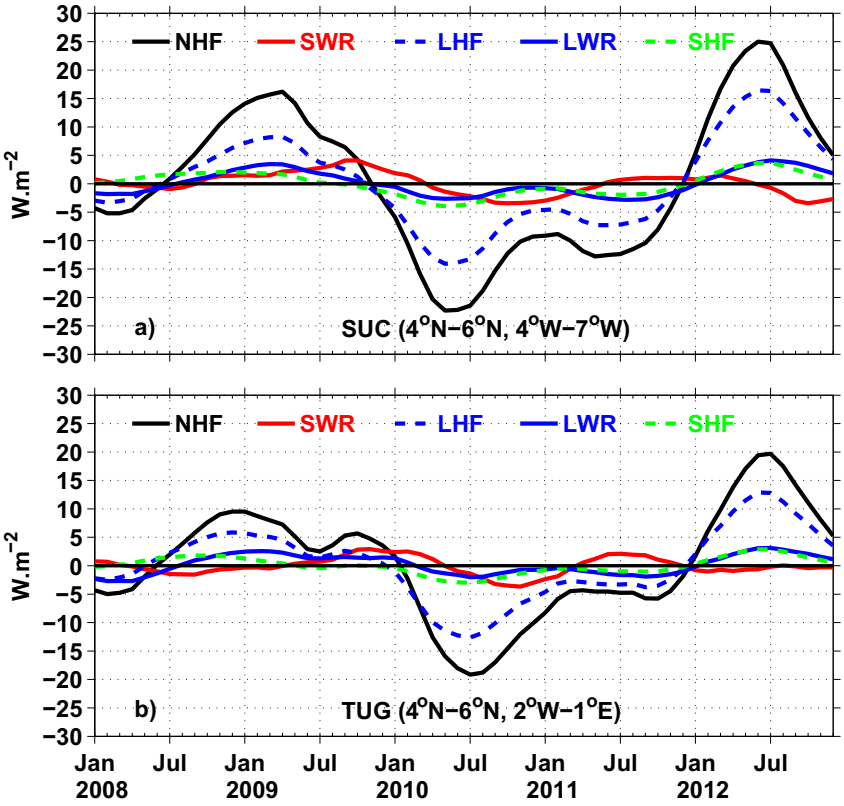

Figure 10. (a) Interannual anomalies of atmospheric fluxes for 2008–2012 period in the Sassandra Upwelling area in Côte d'Ivoire region: total net atmospheric forcing (NHF, black), shortwave radiation (SWR, red), latent heat flux (LHF, dashed blue), longwave radiation (LWR, blue) and sensible heat flux (SHF, dashed green). (b) Same as (a) but for the Takoradi Upwelling area in Ghana region. The units are W.m^{-2}.

from its seasonal climatology (Figure 8). The contribution of HAD to the SST cold event was dominated by changes in zonal advection (XAD) caused by changes in the zonal SST gradient (Figure 9). The changes in the NHF term showed that it was opposed to cooling throughout 2012. From July 2012, the warming created by the NHF managed to stop the cooling and the SST started to increase until the end of 2012 (Figure 7a). The anomalous warming from NHF that occurred in 2012 was largely due to positive anomalies in the latent heat flux (LHF; Figure 10a), corresponding to a reduction of this cooling term. It has been demonstrated that changes in LHF in the SUC are mostly related to changes in the vertical humidity gradient which results from the changes in SST (e.g., Foltz & McPhaden, 2006b).

In summary, in the SUC region, the February–June 2012 SST cold event was largely explained by an enhanced vertical mixing caused by the increased vertical shear driven by the strengthened Guinea Current, in the presence of weak stratification at the base of the mixed-layer. A secondary contribution comes from changes in zonal advection, resulting from changes in the zonal SST gradient. In this region, the increase in net heat flux due to the diminution of the latent heat flux stopped this cooling and the SST started to increase from July until the end of 2012.

For the TUG region, as for the SUC, between the end of 2011 and the middle 2012, anomalous SST cooling was important with maximum SST anomaly of ~ -0.75°C observed in June 2012 (Figures 11a). Note that in 2012 the 20°C isotherm depth was shallower than usual and the sea surface height showed a relative minimum at the same time, while not the largest of the 2008–2012 period (not shown). This again suggests that there is no direct link between the SST cooling and change in upwelling strength. The total temperature tendency term that resulted from the sum of NHF and OCP was small because these two terms, although having high interannual variability, were opposite all the time. As in SUC, a very strong correlation ($r = +0.96$, significant at the 99% level) was found between OCP and SST anomalies, strongly suggesting

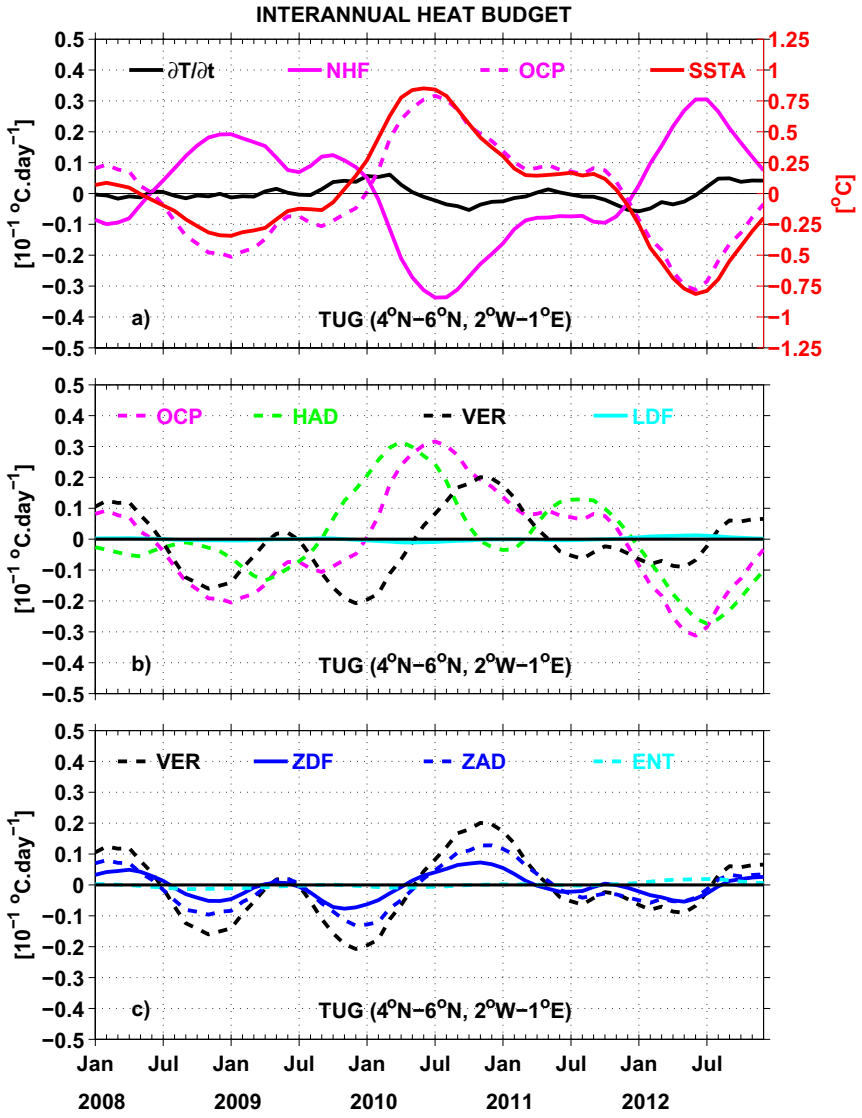

Figure 11. Same as Figure 7 but for the Takoradi Upwelling area in Ghana region.

that this term was the source of the cold SST event in 2012. Contrary to the SUC region where the term ZDF was important to explain the 2012 SST cooling, in the TUG region, the contribution of this term was small and the OCP term was mainly determined by HAD (Figures 11b and 11c). By decomposing HAD into its zonal and meridional components, we found that HAD was essentially dominated by meridional advection (YAD) in 2012 (Figure 12a). The changes in YAD was driven by the southward anomaly (acceleration) of the meridional Ekman current that resulted from the strengthening of the zonal wind stress recorded in 2012 (Figures 12b and 12c; Figure 1b). As in SUC, NHF was not involved in the cooling of the SST during February-June 2012 and the changes in NHF in this period were primarily dominated by the decrease in LHF (Figure 10b). The reduction of LHF in the TUG region is associated, like in the SUC, with changes in the vertical humidity gradient resulting from the SST changes (e.g., Foltz & McPhaden, 2006b). From July 2012, NHF dominated the term that created the cooling (YAD) and SST started to increase until the end of 2012.

To summarize, in the TUG region, anomalous meridional advection was mostly responsible for the February-June 2012 cooling of the SST. The changes in meridional advection, in this period, were attributed to the southward acceleration of the meridional Ekman current caused by the intensification of the zonal wind stress. Finally, the NHF driven by the reduction of LHF stopped the cooling from July 2012 and the SST increased until the end of this year.

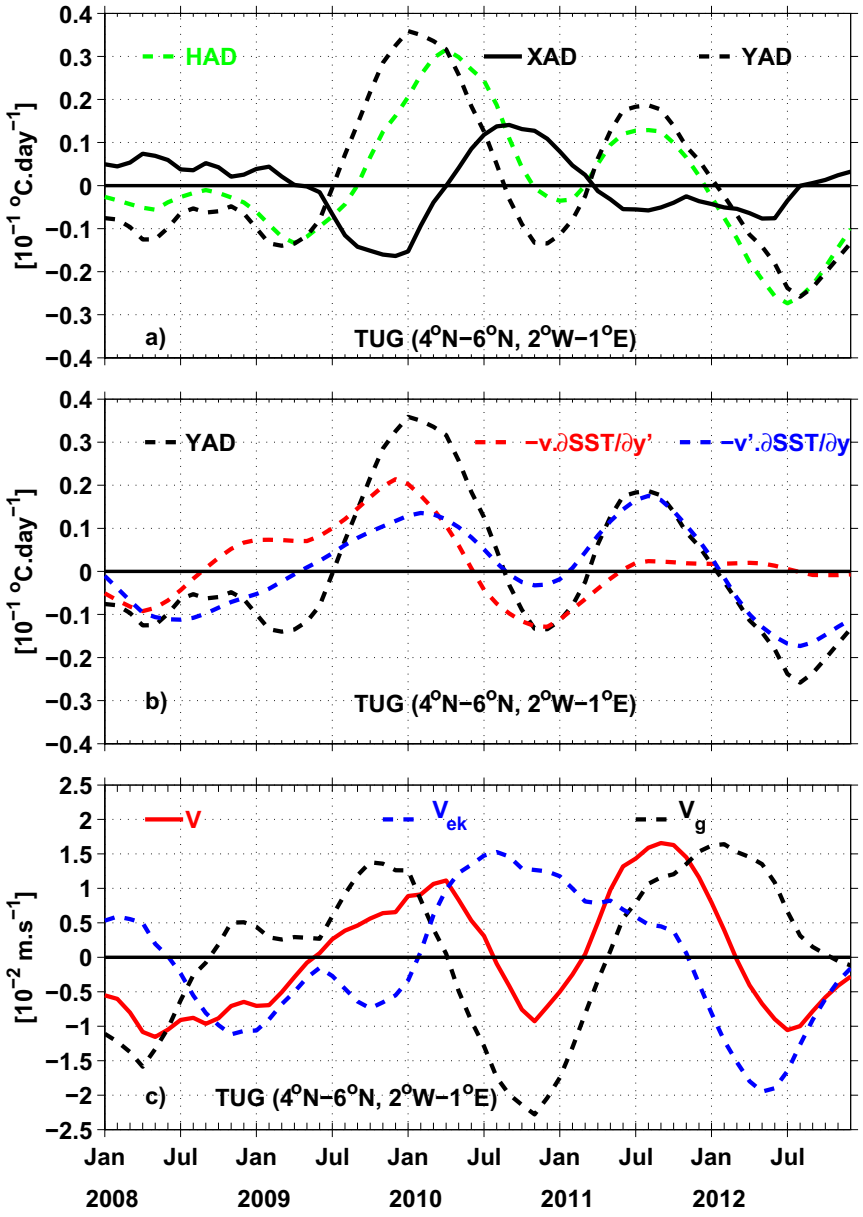

Figure 12. Interannual anomalies for 2008–2012 in the Takoradi Upwelling area in Ghana region for (a) decomposition of horizontal advection (HAD, dashed green) into zonal (XAD, black) and meridional (YAD, dashed black) components; (b) meridional advection (dashed black, same as the dashed black line in a), meridional advection caused by the meridional sea surface temperature (SST) gradient anomalies (dashed red) and meridional advection created by the meridional current anomalies (dashed blue); and (c) decomposition of meridional current (V, red) into geostrophic (Vg, dashed black) and Ekman currents (Vek, dashed blue). All terms are in °C. day^{-1} for (a and b), and in m. s^{-1} for (c).

4. Summary and Discussion

During February-June, SST reaches its seasonal maximum in the Northern Gulf of Guinea (NGoG), but in 2012 it was anomalously cold. The most pronounced cold SST anomalies observed in 2012 reached −1°C in the SUC and −0.5°C in TUG. The causes of the SST cooling are examined using a model mixed-layer heat budget.

We have shown that, in the SUC region, this cold SST event was caused by changes in both vertical mixing at the base of the mixed-layer and zonal advection. The changes in vertical mixing were induced by strong

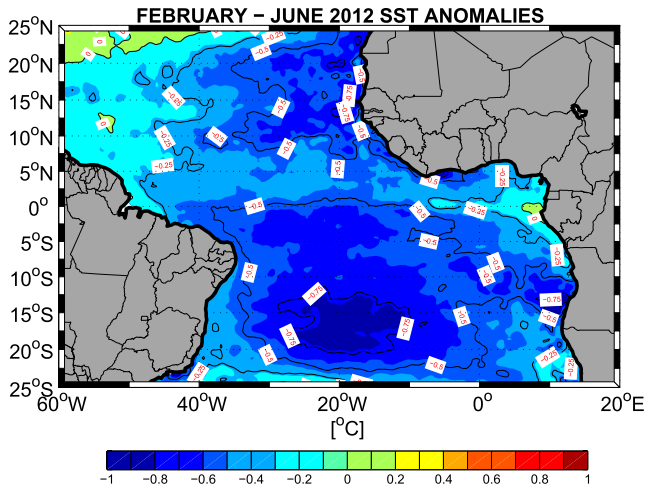

Figure 13. February–June 2012 Optimum Interpolation-sea surface temperature anomalies in the tropical Atlantic. The units is °C.

vertical shear of zonal currents driven by the Guinea Current strengthening in the presence of weak stratification at the base of the mixed-layer, while zonal advection changes were associated with an anomalous zonal gradient of SST. In the TUG region, changes in the meridional advection were mainly involved in the 2012 SST cooling. The changes in meridional advection were driven by the southward acceleration of the meridional Ekman current that was created by the intensification of the zonal wind stress. In these two regions (SUC and TUG), changes (increase) in net heat flux were largely dominated by a reduction in latent heat flux, a negative feedback driven by the SST cooling (e.g., Foltz & McPhaden, 2006b), and this term played an important role in the termination of the SST cold event. These results reveal that, as for the boreal summer coastal upwelling in the NGoG (Djakouré et al., 2017), the mechanisms responsible for the decrease in SST differ in the two regions.

Previous studies have indicated that the 2012 cooling may be associated with interannual Atlantic climatic modes (Sohou et al., 2020). It is interesting to remark that the period of appearance of the strong cooling (February–June) in 2012 does not correspond with the period when the Atlantic Niño mode (or equatorial mode) normally reaches its peak amplitude (June-July-August). In addition, a study based on observations over the period 1979–2016 has found that there was no Atlantic Niño in 2012 in the Gulf of Guinea (Awo et al., 2018). Thus, these results indicate that the abnormally cold SST event observed in February–June 2012 cannot be related to the main mode of interannual variability of the Gulf of Guinea. It has been established that the Atlantic meridional mode (or Atlantic dipole) is thermodynamic in nature due to the important role played by air-sea heat fluxes, mainly the changes in latent heat flux induced by wind anomalies, driven themselves by SST anomalies (Chang et al., 2001; Foltz & McPhaden, 2010). In the NGoG region, latent heat flux changes were not related to wind anomalies but to changes in the vertical humidity gradient as a consequence of SST changes. Although the air-sea heat flux changes were largely dominated by the changes in the latent heat flux, we showed that the latent heat flux anomalies were not involved in the development of the 2012 SST cold event. Therefore, these results suggested that the meridional mode, which was active in spring 2012 (Awo et al., 2018), may not be the main source of the cold event of 2012. Jouanno et al. (2017) have indicated that ocean dynamics, driven by the winds, played an important role in the interannual variability of the SST in the coastal upwelling areas of NGoG. This study also revealed that ocean dynamics, forced by wind stress changes, were responsible for the SST cold event during February–June 2012. The role of vertical mixing anomalies in the development of SST changes in the NGoG region has been also suggested by Wade et al. (2011). Although this term was the driving factor behind the 2012 SST cooling (negative SST anomalies) in the SUC region, this was not the case in the TUG region where the anomalies of meridional Ekman current was identified as the main cause of the 2012 SST cold event.

In the western tropical Atlantic Ocean, using observational data, a strong cooling of the SST was also observed between March and May 2012 by Nogueira Neto et al. (2018). These authors have explained this cold SST event by the latent heat flux anomalies due to anomalous wind stress, whereas we showed, in the present study, that latent heat flux anomalies were not at the origin of the 2012 SST cooling in the NGoG. These results indicate that the strong cooling of 2012 was not only observed in the NGoG region but was also recorded in the western tropical Atlantic and the causes of the SST cooling in the NGoG differ from those found in the western tropical Atlantic. Figure 13 reveals that the whole tropical Atlantic region was affected by the 2012 SST cooling with the strongest SST anomalies values exceeding 1°C in three distinct regions: the Southwestern tropical Atlantic (12.5°S–20°S; 10°W–25°W), the Angola upwelling area (12.5°S–16°S, 10°E–14°E) and our region of focus in the NGoG. Nogueira Neto et al. (2018) study in the western tropical Atlantic covers the area between 20°S and 20°N; 15°W–60°W of strong negative SST anomalies located in the Southwestern tropical Atlantic. However, the strong cooling of the SST located at the Angola upwelling remains to be investigated.

Although our study focused on the cold event of 2012, we also noted over our study period, both in the model and observations, the 2010 warm SST event in the NGoG. This warm event has been discussed by Lefèvre et al. (2013) and the weakening of the trade winds has been suggested as the origin of the SST warming. In the present study, Figure 6 showed that in the SUC region, both decreases in the cooling effect of vertical mixing and vertical advection caused the 2010 warming of the SST. The decrease in vertical mixing was related to the weakening of the vertical shear caused by the weakening of the Guinea Current in the presence of a strong stratification at the base of the mixed-layer (Figure 8). The decrease in vertical advection was driven by the weakening of the vertical velocity (not shown). For the TUG region, only changes in the meridional advection due to changes in both onshore geostrophic and Ekman meridional currents were responsible for the warm SST event in 2010 (Figures 11 and 12). Changes in the onshore meridional geostrophic current are caused by the alongshore sea surface height anomalies (Alory et al., 2021) while the changes in meridional Ekman current are due to the weakening of the zonal wind stress (not shown). All these findings highlight the major role played by wind stress changes in the 2010 SST warming and are in agreement with the suggestions of Lefèvre et al. (2013).

Data Availability Statement

The ERA Interim reanalysis data were downloaded from the European Center for Medium-Range Weather Forecasts website (http://www.ecmwf.int) and the OI-SST data were provided by National Oceanic and Atmospheric Administration (NOAA) website (https://www.esrl.noaa.gov/psd/). Note that ONSET in-situ data and the Model outputs are available on demand.

Acknowledgments
The authors acknowledge the financial support of the EU H2020 TRIATLAS project under Grant Agreement 817578. This work is also in the framework of the Jeune Equipe Associée à l'IRD (JEAI) named Variabilité de la SAlinité et Flux d'eau doUce à Multi-Échelles (SAFUME) which is supported by IRD. The authors thank the anonymous reviewers for their comments and suggestions that helped improved the manuscripts.

References

Ali, K., Kouadio, K., Zahiri, G., Aman, A., Assamoi, A., & Bourlès, B. (2011). Influence of the Gulf of Guinea coastal and equatorial upwellings on the precipitations along its northern coasts during the boreal summer period. *Asian Journal of Applied Sciences*, *4*(3), 271–285. https://doi.org/10.3923/ajaps.2011.271.285

Alory, G., Da-Allada, C. Y., Djakouré, S., Dadou, I., Jouanno, J., & Loemba, D. P. (2021). Coastal upwelling limitation by onshore geostrophic flow in the Gulf of Guinea around the Niger River Plume. *Frontiers in Marine Science*, *7*, 1116. https://doi.org/10.3389/fmars.2020.607216

Awo, F. M., Alory, G., Da Allada, Y. C., Delcroix, T., Jouanno, J., & Baloitcha, E. (2018). Sea surface salinity signature of the tropical Atlantic interannual climatic modes. *Journal of Geophysical Research: Oceans*, *123*. 7420–7437. https://doi.org/10.1029/2018JC013837

Binet, D., & Marchal, E. (1993). The large marine ecosystem of shelf areas in the Gulf of Guinea: Long-term variability induced by climatic changes. In K. Sherman, L. M. Alexander, & B. D. Gold (Eds.), *Large marin ecosystems: Storn, mitigation and sustainability* (pp. 104–118). AAAS Publication 92-395.

Burmeister, K., Brandt, P., & Lubbecke, J. F. (2016). Revisiting the cause of the eastern equatorial Atlantic cold event in 2009. *Journal of Geophysical Research: Oceans*, *121*, 4777–4789. https://doi.org/10.1002/2016JC011719

Chang, P., Ji, L., Li, H., & Flügel, M. (1997). A decadal climate variation in the tropical Atlantic Ocean from thermodynamic air–sea interactions. *Nature*, *385*(6616), 516–518. https://doi.org/10.1038/385516a0

Chang, P., Ji, L., & Saravanan, R. (2001). A hybrid coupled model study of tropical Atlantic variability. *Journal of Climate*, *14*(3), 361–390. https://doi.org/10.1175/1520-0442(2001)013<0361:AHCMSO>2.0.CO;2

Da-Allada, C. Y., Jouanno, J., Gaillard, F., Kolodziejczyk, N., Maes, C., Reul, N., & Bourlès, B. (2017). Importance of the Equatorial Undercurrent on the sea surface salinity in the Eastern Equatorial Atlantic in boreal spring. *Journal of Geophysical Research: Oceans*. https://doi.org/10.1002/2016JC012342

Da-Allada, Y. C., du Penhoat, Y., Jouanno, J., Alory, G., & Hounkonnou. (2014). Modeled mixed-layer salinity balance in the Gulf of Guinea: Seasonal and interannual variability. *Ocean Dynamics*. https://doi.org/10.1007/s10236-014-0775-9

Dai, A., & Trenberth, K. (2002). Estimates of freshwater discharge from continents: Latitudinal and seasonal variations. *Journal of Hydrometeorology*, *3*, 660–687. https://doi.org/10.1175/1525-7541(2002)003<0660:EOFDFC>2.0.CO;2

de Boyer Montégut, C., Madec, G., Fischer, A. S., Lazar, A., & Iudicone, D. (2004). Mixed layer depth over the global ocean: An examination of profile data and a profile-based climatology. *Journal of Geophysical Research*, *109*, C12003. https://doi.org/10.1029/2004JC002378

Dee, D. P., Uppala, S. M., Simmons, A. J., Berrisford, P., Poli, P., Kobayashi, S., et al. (2011). The ERA-Interim reanalysis: Configuration and performance of the data assimilation system. *Quarterly Journal of the Royal Meteorological Society*, *137*, 553–597. https://doi.org/10.1002/qj.828

Djakouré, S., Penven, P., Bourlès, B., Koné, V., & Veitch, J. (2017). Respective roles of the Guinea current and local winds on the coastal upwelling in the Northern Gulf of Guinea. *Journal of Physical Oceanography*, *47*(6), 1367–1387. https://doi.org/10.1175/jpo-d-16-0126.1

Djakouré, S., Penven, P., Bourlès, B., Veitch, J., & Koné, V. (2014). Coastally trapped eddies in the north of the Gulf of Guinea. *Journal of Geophysical Research: Oceans*, *119*, 6805–6819. https://doi.org/10.1002/2014jc010243

Dussin, R., Barnier, B., & Brodeau, L. (2016). Up-dated description of the DFS5 forcing data set: The making of Drakkar forcing set DFS5. In *DRAKKAR/MyOcean Rep. 01-04-16*. Grenoble, France. Laboratory of Glaciology and Geophysics of the Environment.

Ferry, N., Parent, L., Garric, G., Bricaud, C., Testut, C.-E., Galloudec, O. L., et al. (2012). GLORYS2V1 global ocean reanalysis of the altimetric era (1992–2009) at mesoscale. *Mercator Ocean–Quaterly Newsletter*, *44*, 29–39.

Foltz, G. R., & McPhaden, M. J. (2006a). Unusually warm sea surface temperatures in the tropical North Atlantic during 2005. *Geophysical Research Letters*, *33*, L19703. https://doi.org/10.1029/2006GL027394

Foltz, G. R., & McPhaden, M. J. (2006b). The role of oceanic heat advection in the evolution of tropical North and South Atlantic SST anomalies, *Journal of Climate*, *19*, 6122–6138. https://doi.org/10.1175/JCLI3961.1

Foltz, G. R., & McPhaden, M. J. (2010). Interaction between the Atlantic meridional and Niño modes. *Geophysical Research Letters*, *37*, L18604. https://doi.org/10.1029/2010GL044001

Gu, G., & Adler, R. F. (2004). Seasonal evolution and variability associated with the West African Monsoon System. *Journal of Climate*, *17*(17), 3364–3377. https://doi.org/10.1175/1520-0442(2004)017<3364:SEAVAW>2.0.CO;2

Hardman-Mountford, N. J., & McGlade, M. (2003). Seasonal and inter-annual variability of oceanographic processes in the Gulf of Guinea: An investigation using AVHRR sea surface temperature data. *International Journal of Remote Sensing*, *24*(16), 3247–3268. https://doi.org/10.1080/0143116021000021297

Hernandez, O., Jouanno, J., & Durand, F. (2016). Do the Amazon and Orinoco freshwater plumes really matter for hurricane-induced ocean surface cooling? *Journal of Geophysical Research: Oceans*, *121*, 2119–2141. https://doi.org/10.1002/2015JC011021

Jouanno, J., Hernandez, O., & Sanchez-Gomezet, E. (2017). Equatorial Atlantic inter-annual variability and its relation to dynamic processes. *Earth System Dynamics*, *8*, 1061–1069. https://doi.org/10.5194/esd-8-1061-2017

Jouanno, J., Marin, F., Penhoat, Y. D., Molines, J.-M., & Sheinbaum, J. (2011). Seasonal modes of surface cooling in the Gulf of Guinea. *Journal of Physical Oceanography*, *41*, 1408–1416. https://doi.org/10.1175/JPO-D-11-031.1

Koné, V., Lett, C., Penven, P., Bourlès, B., & Djakouré, S. (2017). A biophysical model of S. aurita early-life history in the northern Gulf of Guinea. *Progress in Oceanography*, *151*, 83–96. https://doi.org/10.1016/j.pocean.2016.10.008

Kouadio, Y., Djakouré, S., Aman, A., Ali, K. E., Koné, V., & Toualy, E. (2013). Characterization of the boreal summer upwelling at the northern Coast of the Gulf of Guinea based on the PROPAO in situ measurements network and satellite data. *International Journal of Oceanography*. 1–11. https://doi.org/10.1155/2013/816561

Lamb, P. J. (1972). Large-scale Tropical Atlantic circulation patterns associated with Sub-Saharan weather anomalies. *Tellus*, *30*, 240–251.

Large, W. G., & Yeager, S. (2009). The global climatology of an interannually varying air–sea flux data set. *Climate Dynamics*, *33*, 341–364. https://doi.org/10.1007/s00382-008-0441-3

Lefèvre, N., Caniaux, G., Janicot, S., & Gueye, A. K. (2013). Increased CO_2 outgassing in February-May 2010 in the tropical Atlantic, following the 2009 Pacific El Niño. *Journal of Geophysical Research: Oceans*, *118*, 1–13. https://doi.org/10.1002/jgrc.20107

Li, Y., Wang, F., & Han, W. (2013). Interannual sea surface salinity variations observed in the tropical North Pacific Ocean. *Geophysical Research Letters*, *40*, 2194–2199. https://doi.org/10.1002/grl.50429

Lübbecke, J. F., & McPhaden, M. J. (2013). A comparative stability analysis of Atlantic and Pacific Niño modes. *Journal of Climate*, *26*, 5965–5980. https://doi.org/10.1175/JCLI-D-12-00758.1

Madec, G., & the NEMO Team. (2016). *NEMO ocean engine, Note du Pôle de Modélisation 27*. Paris. Institut Pierre-Simon Laplace.

Nogueira Neto, A. V., Giordani, H., Caniaux, G., & Araujo, M. (2018). Seasonal and interannual mixed-layer heat budget variability in the western tropical Atlantic from Argo floats (2007-2012). *Journal of Geophysical Research: Oceans*, *123*, 5298–5532. https://doi.org/10.1029/2017JC013436

Opoku-Ankomah, Y., & Cordery, I. (1994). Atlantic sea surface temperatures and rainfall variability in Ghana. *Journal of Climate*, *7*, 551–558. https://doi.org/10.1175/1520-0442(1994)007<0551:ASSTAR>2.0.CO;2

Picaut, J. (1983). Propagation of the seasonal upwelling in the eastern equatorial Atlantic. *Journal of Physical Oceanography*, *13*, 18–37. https://doi.org/10.1175/1520-0485(1983)013<0018:POTSUI>2.0.CO;2

Reffrary, G., Bourdalle-Badie, R., & Calone, C. (2015). Modelling turbulent vertical mixing sensitivity using a 1-D version of NEMO. *Geoscientific Model Development*, *8*, 69–86. https://doi.org/10.5194/gmd-8-69-2015

Reynolds, R. W., Rayner, N. A., Smith, T. M., Stokes, D. C., & Wang, W. (2002). An improved in situ and satellite SST analysis for climate. *Journal of Climate*, *15*, 1609–1625. https://doi.org/10.1175/1520-0442(2002)015<1609:AIISAS>2.0.CO;2

Reynolds, R. W., Smith, T. M., Liu, C., Chelton, D. B., Casey, K. S., & SchlaxMG. (2007). Daily high resolution blended analysis for sea surface temperature. *Journal of Climate*, *20*, 5473–5496. https://doi.org/10.1175/2007JCLI1824.1

Roy, C. (1995). The Côte d'Ivoire and Ghana coastal upwelling dynamics and changes. In X. Bard, & K. A. Koranteng (Eds.), *Dynamics and use of sardinella resources from upwellling off Ghana and Ivory Coast* (pp. 346–361). Paris. ORSTOM Editions.

Servain, J., Picaut, J., & Merle, J. (1982). Evidence of remote forcing in the equatorial Atlantic Ocean. *Journal of Physical Oceanography*, *12*, 457–463. https://doi.org/10.1175/1520-0485(1982)012<0457:EORFIT>2.0.CO;2

Sohou, Z., Koné, V., Da-Allada, Y. C., Djakouré, S., Bourlès, B., Racape, V., et al. (2020). Seasonal and inter-annual ONSET sea surface temperature variability along the northern coast of the Gulf of Guinea. *Regional Studies in Marine Science*, *35*, 101129. https://doi.org/10.1016/j.rsma.2020.101129

Toualy, E., Stanojevic, G., Kouadio, K., & Aman, A. (2012). Multi-decadal variability of sea surface temperature in the northern coast of the Gulf of Guinea. Asian Journal of Applied Sciences. ISSN 1996-3343. In J.-M. Verstraete (Eds.), *The seasonal upwellings in the Gulf of Guinea. Progress in Oceanography*, 29, 1–60.

Umlauf, L., & Burchard, H. (2003). A generic length-scale equation for geophysical turbulence models. *Journal of Marine Research*, *61*(31), 235–265. https://doi.org/10.1357/002224003322005087

Vialard, J., Menkes, C., Boulanger, J. P., Delecluse, P., & Guilyardi, E. (2001). A model study of oceanic mechanisms affecting equatorial pacific sea surface temperature during the 1997–1998 EL Nino. *Journal of Physical Oceanography*, *31*, 1649–1675. https://doi.org/10.1175/1520-0485(2001)031<1649:AMSOOM>2.0.CO;2

Wade, M., Caniaux, G., & du Penhoat, Y. (2011). Variability of the mixed layer heat budget in the eastern equatorial Atlantic during 2005-2007 as inferred using Argo floats. *Journal of Geophysical Research*, *116*, C08006. https://doi.org/10.1029/2010JC006683

Zebiak, S. E. (1993). Air-sea interaction in the equatorial Atlantic region. *Journal of Climate*, *6*, 1567–1586. https://doi.org/10.1175/1520-0442(1993)006<1567:AIITEA>2.0.CO;2